



Original Articles

Loss of TGF- β signaling in osteoblasts increases basic-FGF and promotes prostate cancer bone metastasis

Xiangqi Meng ^{a, b}, Alexandra Vander Ark ^a, Paul Daft ^a, Erica Woodford ^a, Jie Wang ^{a, c}, Zachary Madaj ^d, Xiaohong Li ^{a,*}

^a Program for Skeletal Disease and Tumor Microenvironment, Center for Cancer and Cell Biology, Van Andel Research Institute, Grand Rapids, MI 49503, USA

^b Sun Yat-sen University Sixth Affiliated Hospital, Guangzhou, 510655, China

^c Radiation Department, Dalian Municipal Central Hospital, Dalian, 116033, China

^d Bioinformatics & Biostatistics Core, Van Andel Research Institute, Grand Rapids, MI 49503, USA

ARTICLE INFO

Article history:

Received 13 December 2017

Received in revised form

2 January 2018

Accepted 8 January 2018

Keywords:

Prostate cancer bone metastasis

Osteoblasts

Osteoclasts

TGF- β signaling

TGF- β type II receptor (TGFBR2)

bFGF

ABSTRACT

TGF- β plays a central role in prostate cancer (PCa) bone metastasis, and it is crucial to understand the bone cell-specific role of TGF- β signaling in this process. Thus, we used knockout (KO) mouse models having deletion of the *Tgfb2* gene specifically in osteoblasts (*Tgfb2*^{Col1CreERT} KO) or in osteoclasts (*Tgfb2*^{LysMCre} KO). We found that PCa-induced bone lesion development was promoted in the *Tgfb2*^{Col1CreERT} KO mice, but was inhibited in the *Tgfb2*^{LysMCre} KO mice, relative to their respective control *Tgfb2*^{FlxoxE2} littermates. Since metastatic PCa cells attach to osteoblasts when colonized in the bone microenvironment, we focused on the mechanistic studies using the *Tgfb2*^{Col1CreERT} KO mouse model. We found that bFGF was upregulated in osteoblasts from PC3-injected tibiae of *Tgfb2*^{Col1CreERT} KO mice and correlated with increased tumor cell proliferation, angiogenesis, amounts of cancer-associated fibroblasts and osteoclasts. *In vitro* studies showed that osteoblastogenesis was inhibited, osteoclastogenesis was stimulated, but PC3 viability was not affected, by bFGF treatments. Lastly, the increased PC3-induced bone lesions in *Tgfb2*^{Col1CreERT} KO mice were significantly attenuated by blocking bFGF using neutralizing antibody, suggesting bFGF is a promising target inhibiting bone metastasis.

© 2018 Elsevier B.V. All rights reserved.

1. Introduction

Bone metastases have been found in 70–90% of the patients who die of prostate cancer (PCa) [1]. It is known that metastatic cancer cells secrete factors such as parathyroid hormone-related protein (PTHrP) that regulate osteoblasts to stimulate the maturation of osteoclasts. Osteoclasts resorb bones to release growth factors such as transforming growth factor beta (TGF- β) from the bone matrix. These factors in turn promote further tumor growth and bone destruction in a “vicious cycle” [2–6]. However, the bone cell-specific role of TGF- β signaling in PCa bone metastases is not clear.

TGF- β signaling occurs when ligand binds to the TGF- β type II receptor (TGFBR2). Upon ligand binding, TGFBR2 phosphorylates TGFBR1, which further phosphorylates the Smad transcription

factor to activate downstream TGF- β /Smad signaling [7]. Therefore, to answer these questions, we used genetically engineered mouse models with deletion of the TGFBR2 in osteoblasts, *Tgfb2*^{Col1CreERT} knock-out (KO), or in osteoclasts, *Tgfb2*^{LysMCre} KO. These mice were crossed to *Rag-2* knockout immunodeficient mice (*Rag2*^{-/-}) so that they were able to grow human tumors. Intratibial or intracardiac PCa cell injections were used for our studies of bone metastases [8]. We found that the bone lesions developed from PC3 PCa cells were significantly promoted in *Tgfb2*^{Col1CreERT} KO mice, but inhibited in *Tgfb2*^{LysMCre} KO mice, relative to those in their respective control *Tgfb2*^{FlxoxE2} mice, suggesting a metastasis-promoting role of TGF- β signaling loss in osteoblasts, and a metastasis-inhibiting role of TGF- β signaling loss in osteoclasts.

It is also known that metastatic PCa cells attach to osteoblasts in order to establish growth in the bone microenvironment [9]. However, the contributions of osteoblasts to bone metastasis are not clear and we need to identify a better target blocking these effects. Using the *Tgfb2*^{Col1CreERT} KO mouse model, we identified basic fibroblast growth factor (bFGF) as the mediator of the

* Corresponding author. Van Andel Research Institute, 333 Bostwick Ave., N.E., Grand Rapids, MI 49503, USA.

E-mail address: xiaohong.li@vai.org (X. Li).

metastasis-promoting effect from osteoblasts. Furthermore, we dissected the functional role of bFGF on bone cells and PC3 cells. bFGF treatments were shown to promote osteoclastogenesis, inhibit osteoblastogenesis, but had no direct effect on PC3 cell viabilities *in vitro*.

Altogether, our study defined a PCa metastasis-promoting effect from loss of TGF- β signaling in osteoblasts, delineated the mechanism of its action, and identified bFGF as a potential target that could block this effect.

2. Materials and methods

2.1. Cells, animals, and reagents

The PCa cell lines PC3 and DU145 were purchased from the American Type Culture Collection (ATCC; Manassas, VA) and were cultured in RPMI-1640 supplemented with 10% fetal bovine serum (FBS).

Tgfb2^{FloxE2} mice [10] were bred with *Col1a*^{CreERT} mice [11] or *Lysm*^{Cre} mice to generate *Tgfb2*^{Col1CreERT}, or *Tgfb2*^{LysmCre} KO [12] mice, respectively. These mice were further bred to mT/mG (JAX, 007676) reporter mice for the visualization of Cre activity, and to *Rag-2* (JAX, 008449) KO mice, whose immunodeficiency allows for the inoculation of human cells. All of the mice were bred, maintained, and used in this study with approval of the VARI Institutional Animal Care and Use Committee and the Department of Defense Prostate Cancer Research Program (DOD PCRP) Animal Care and Use Committee. The breeding (1 male and 2 females per cage) and maintaining (4 males or 5 females per cage) of these mice were kept in a specific pathogen free barrier facility. The experimental mice were transferred to a conventional, non-barrier space for all the procedures and were euthanized at endpoint for tissue analyses.

Details of the reagents used in the studies, including the catalogue, doses, and applications, are listed in [Supplemental Table 1](#).

2.2. Injections and radiographic imaging

To generate the *Tgfb2*^{Col1CreERT} KO mice, Cre-positive male mice at age 4–5 weeks were intraperitoneally (*i.p.*) injected with tamoxifen (40 µg/g body weight) for 5 d. At 5–7 d after the last injection, the mice were randomly allocated for treatment. The Cre-negative littermates were treated the same as the Cre-positive mice and served as *Tgfb2*^{FloxE2} control mice. For intratibial injections, one million PC3 or DU145 PCa cells in 10 µl of PBS were injected into the left tibia, and 10 µl of PBS was injected into the contralateral tibia as a control. For intracardiac injections, 200,000 PC3 cells in 100 µl of PBS were injected per mouse.

Mice were imaged using Biopix piXarray Digital Specimen Radiography (Faxitron Biopix) weekly for bone lesion development. Mice that never developed lesions were considered technical injection failures and were excluded from the studies. No data points from mice with successful injections were excluded from the data set. The bone lesions were counted and areas were measured from X-rays using MetaMorph (Molecular Devices, Inc.). All defined regions of interest (ROIs) were analyzed. The cell preparations, injections, imaging, and bone lesion analysis were performed blinded by individuals of our lab.

Mouse tibiae were harvested in 70% ethanol and subjected to microcomputed tomography (µCT) scanning and imaging using a SKYSCAN 1172 µCT instrument (Bruker, Ettlingen, Germany). The trabecular ROI extended 8 mm from the subchondral plate in the distal direction in order to include all potential tumor areas. SkyScan software (DataViewer, CTAn, and CTVox) was used to determine the three-dimensional structural parameters, including BV/

TV, Tb.Th, Tb.Sp, Tb.N, BMD, mean total cross-sectional bone perimeter (B.Pm), average object equivalent circle diameter per slice (Av.Obj.ECD), and cross-sectional thickness (Cs.Th). All measured variables in the left tibiae with PCa were normalized to right tibiae.

2.3. Histological and histomorphometry analyses

Mouse tibiae were harvested, fixed, processed, sectioned, stained, and analyzed as previously described [12,13]. Sections were stained for TRAP and with H&E to confirm the osteoclast and osteoblast identity and were subjected to histomorphometry analyses of tumor burden and bone cells using Bioquant system imaging software 2014 (Nashville, TN). IHC or immunofluorescence was performed on the serial sections.

2.4. Protein or RNA extractions, western blots, and qRT-PCR

Tibiae were harvested and snap-frozen in liquid nitrogen and then were homogenized using FastPrep-24 (MP Biomedicals) for protein or total RNA extractions [12]. For western blots, 40 µg of total protein per sample was used. For cytokine arrays, equal amounts of protein per tibia were pooled from three mice (either *Tgfb2*^{FloxE2} or *Tgfb2*^{Col1CreERT} KO littermates) 3 weeks after PC3 tibial injection. qRT-PCR was performed using SYBR Supermix (Bio-Rad, Hercules, CA) on the ABI machine. Primers were custom-synthesized (IDT, Coralville, IA). The sequences of the primers are listed in [Supplemental Table 2](#).

2.5. Bone marrow differentiation

For osteoblastogenesis, mouse bone marrow cells from *Tgfb2*^{FloxE2} mice were used. On the third day of culture, these bone marrow cells were infected with either adeno-Cre or adeno-GFP to generate either *Tgfb2* KO (OB_KO) or *Tgfb2* Flox (OB_Flox) control cells, respectively. These cells were then further differentiated for another 7 d in α-MEM medium supplemented with 10% FBS and 50 µg/ml of ascorbic acid. The media was changed every 3 d until the end of the experiments. Alkaline phosphatase (ALP) staining was performed.

For osteoclastogenesis, the bone marrow cells from either *Tgfb2*^{Col1CreERT} KO or *Tgfb2*^{FloxE2} mice were counted and cultured in α-MEM with 30 ng/ml macrophage colony-stimulating factor (MCSF) on the first day. On the second day, the non-adherent cells were collected and replated with αMEM (10% FBS + 30 ng/ml RANKL [receptor activator of nuclear factor kappa-B ligand] + 30 ng/ml MCSF). The medium was then changed every 3 days until day 7 or 8. TRAP staining was performed at the end points.

2.6. Statistical analysis

Longitudinal bone lesion data were analyzed via a linear mixed-effect model. Linear contrasts with a false discovery rate correction were used to test for significant differences in bone lesion growth rates, and bootstrap hypothesis testing with 1000 resampled data sets was used to test for differences in total lesion area between groups at specific time points. For experiments without repeated measures, data were analyzed via two-way ANOVA when there were two independent variables; otherwise, a two-tailed Student's *t*-test was used. Normality assumptions were assessed visually via QQ-plots; no concerning deviations were detected. The incidence of bone lesions was analyzed via log-rank tests. *t*-Tests and ANOVAs were done via Graphpad and all other analyses via R v 3.2.2. For all analyses, *P* < .05, two-sided was considered significant.

3. Results

3.1. Loss of TGF- β signaling in osteoblasts promoted, but in osteoclasts inhibited, PC3 bone lesions

To study the role of TGF- β signaling in osteoblasts in PCa bone metastasis, the genetically engineered mouse model, *Tgfb2^{Col1CreERT}* KO mice were used. The osteoblast-specific Cre expression and activation of the *Tgfb2^{Col1CreERT}* KO mice were confirmed by genotyping and IHC analysis of GFP expression in the mouse tibiae. The expression of the TGF- β signaling downstream transcription factor p-Smad2 was also determined. p-Smad2 was expressed in osteoblasts from *Tgfb2^{FloxE2}* mice tibiae, but loss of p-Smad2 was found in the GFP-positive *Tgfb2^{Col1CreERT}* KO osteoblasts (Fig. 1A). The tibiae from *Tgfb2^{FloxE2}* and *Tgfb2^{Col1CreERT}* KO mice were analyzed using histomorphometry, whole-body X-rays, and microCT (Supplemental Fig. 1); no significant differences were found between the bone tissues of the KO and control littermates. PC3 cells were intracardially injected into these mice. A significant increase of bone lesion development was observed in the *Tgfb2^{Col1CreERT}* KO mice relative to *Tgfb2^{FloxE2}* mice (Fig. 1B–C). H&E staining of the mouse bone confirmed the growth of PC3 tumor in the larger osteolytic bone lesion areas in the *Tgfb2^{Col1CreERT}* KO mice (Fig. 1D). To determine whether there are same effects when PCa cells colonized in the bone microenvironment, PC3 cells were intratibially injected into the mice and the development of bone lesions was monitored. Significantly larger bone lesion areas in the *Tgfb2^{Col1CreERT}* KO mice tibiae relative to *Tgfb2^{FloxE2}* mice were indeed observed at the second, third, and fourth weeks after injection (Fig. 2A). The differences of PC3 bone lesions between *Tgfb2^{Col1CreERT}* KO and *Tgfb2^{FloxE2}* mice were further confirmed

using three-dimensional microCT. We found a significant decrease in the bone volume/tissue volume (BV/TV) ratio and trabecular number (Tb.N), as well as increased trabecular separation (Tb.Sp) in the PC3-injected *Tgfb2^{Col1CreERT}* KO mice tibiae (Fig. 2B). The trabecular thickness (Tb.Th) and bone mineral density (BMD) values were not significantly changed (data not shown). In addition, the increased bone lesion areas in *Tgfb2^{Col1CreERT}* KO mice compared to those from *Tgfb2^{FloxE2}* mice were also observed using DU145, at the 5th and 7th weeks after cancer cell intratibial injections (Supplemental Fig. 2A–C). The median time to bone lesion detection was significantly shorter in *Tgfb2^{Col1CreERT}* KO mice (3 weeks) than 5 weeks in *Tgfb2^{FloxE2}* mice.

On the other hand, to study the role of TGF- β signaling in osteoclasts in bone metastasis, the genetically engineered mouse model, *Tgfb2^{LysMCre}* KO mice were used. In the intratibial injection bone metastasis models, PC3-induced bone lesions were significantly smaller in *Tgfb2^{LysMCre}* KO mice relative to their respective *Tgfb2^{FloxE2}* littermates at the third and fourth weeks after injection (Fig. 2C).

3.2. Loss of TGFBR2 in osteoblasts provided a hospitable bone microenvironment for PC3 tumors

To explore the cellular and molecular mechanism by which loss of TGFBR2 promoted PC3 bone lesions, we performed IHC analysis of CD31 (for angiogenesis) and of phosphorylated histone H3 (p-H3; for proliferation); immunofluorescence analysis (IF) for GFP and alpha-smooth muscle actin (α -SMA); and bone histomorphometry analyses in PC3-injected tibiae. Relative to the *Tgfb2^{FloxE2}* mice, *Tgfb2^{Col1CreERT}* KO mice had significant increases in tumor cell proliferation (1.7-fold increase in positive IHC staining

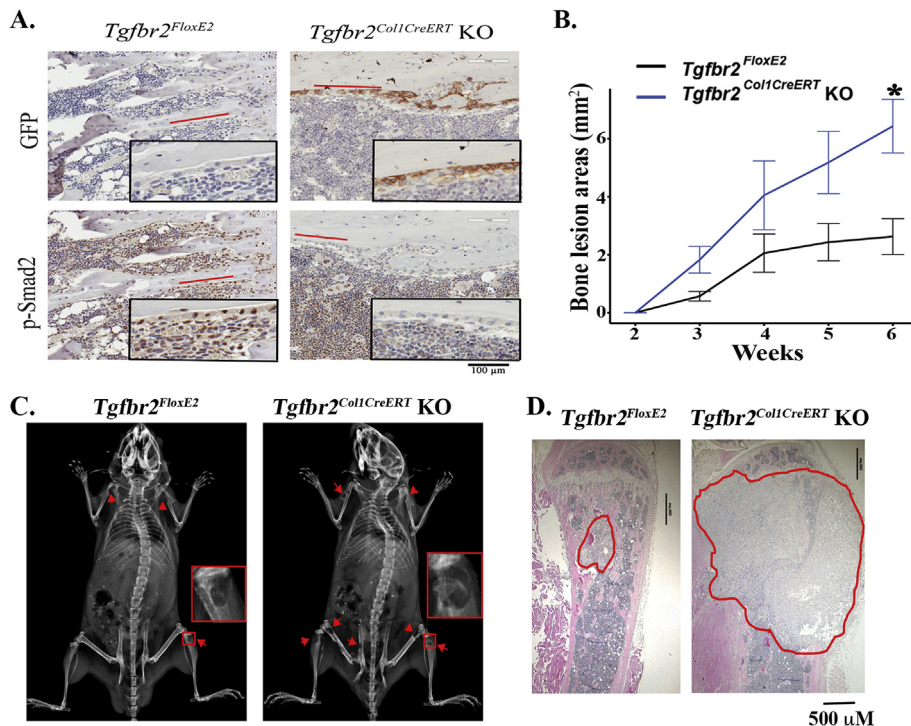


Fig. 1. PC3 bone metastases were promoted in *Tgfb2^{Col1CreERT}* KO mice. **A)** IHC of GFP and p-Smad2. Red lines indicate osteoblasts. IHC was done on serial sections of paraffin embedded mouse tibiae. GFP-positive cells (an indication of Cre activity) were specifically detected in osteoblasts of *Tgfb2^{Col1CreERT}* KO mice, concurrent with the loss of p-Smad2 (scale bar, 100 μ m for the insets). **B)** In the PC3 intracardiac injection model, metastatic bone lesion development was significantly promoted in *Tgfb2^{Col1CreERT}* KO mice than those in *Tgfb2^{FloxE2}* mice (linear mixed-effects model with a random intercept, $*P \leq .05$, $n \geq 4$). **C)** Whole body x-ray images show bone lesions in the mice at 6 wks post PC3 intracardiac injections, indicated by red arrows. **D)** Red outlines indicated the PC3 tumor growth in the bone lesion areas in H&E staining pictures of PC3 metastasized bones at 6 wks post injections.

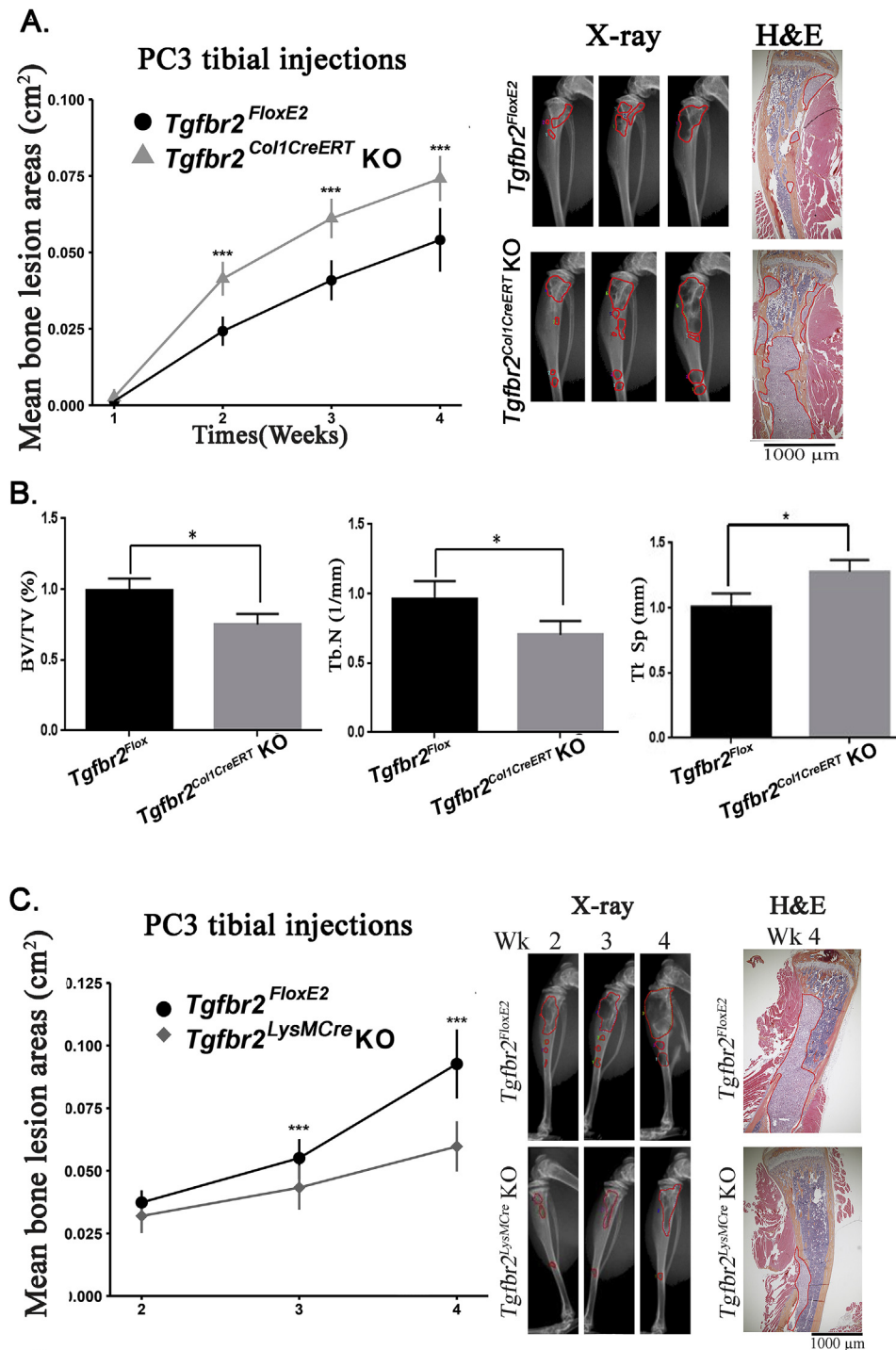


Fig. 2. PC3-induced osteolytic bone lesions were increased in *Tgfb2^{Col1CreERT}* KO mice, but decreased in *Tgfb2^{LysMCre}* KO mice. **A)** Graph shows the mean bone lesion area in PC3-injected mouse tibiae. Significant increases in bone lesion areas were found in *Tgfb2^{Col1CreERT}* KO mice relative to those in *Tgfb2^{FloxE2}* mice (linear mixed-effects model with a random intercept, ***P ≤ .001, n ≥ 10). Red outlines indicated the bone lesion areas measured in the X-ray pictures, and tumor growth in the H&E staining pictures. **B)** Quantitative microCT analyses. Significant decreases in trabecular bone volume/tissue volume (BV/TV), trabecular bone number (Tb.N), but increased trabecular bone separation (Tb.Sp), were found in *Tgfb2^{Col1CreERT}* KO tibiae, relative to tibiae from *Tgfb2^{FloxE2}* mice by student t-test, two-tailed, *P ≤ .05, n ≥ 9. All data were normalized to the contralateral tibia. **C)** Graph shows the mean bone lesion area in PC3-injected mouse tibiae. Significant decreases in bone lesion areas were found in *Tgfb2^{LysMCre}* KO mice relative to those in *Tgfb2^{FloxE2}* mice (linear mixed-effects model with a random intercept, ***P ≤ .001, n ≥ 10). Red outlines indicated the bone lesion areas measured in the X-ray pictures, and tumor growth in the H&E staining pictures.

of PCa cells for p-HH3); microvessel density (2.2-fold increase in CD31-positive microvessels); osteoclastogenesis (5.2-fold increase in tartrate-resistant acid phosphatase [TRAP] staining of osteoclasts); and CAF formation (3.1-fold increase in α-SMA staining

cells) (Fig. 3A–D). These data suggest that loss of TGF-β signaling in osteoblasts has a metastasis-promoting effect on PC3-induced bone lesion development, which is correlated with increases of tumor cell proliferation, angiogenesis, numbers of CAFs and osteoclasts.

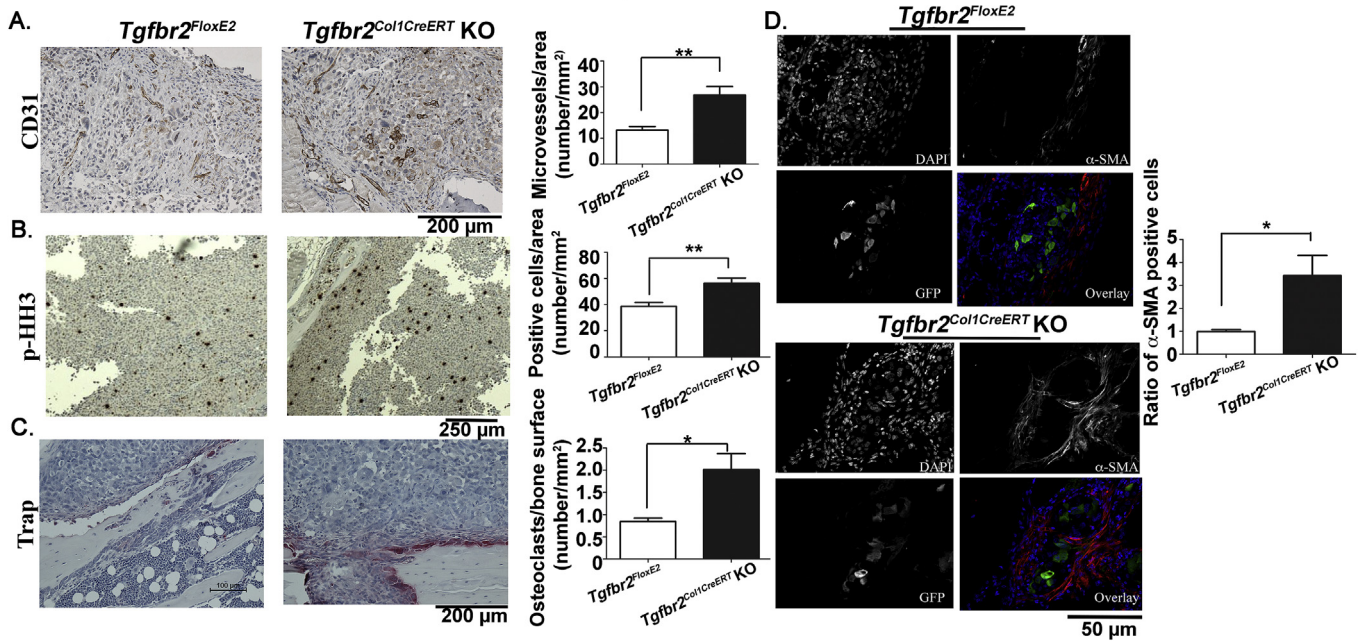


Fig. 3. Proliferation, angiogenesis, cancer-associated fibroblasts, and osteoclasts were increased in PC3-induced bone lesions in *Tgfb2^{Col1CreERT}* KO mice. A-B) Representative IHC staining and quantification of CD31, phosphorylated-histone H3 (P-HH3), and C) representative tartrate-resistant acid phosphatase (TRAP) staining and bone histomorphometry analysis. D) Representative immunofluorescence and quantification of the α -SMA positive fibroblasts, normalized to the number of GFP-positive PC3 cells. *t*-test, two-tailed, **P* ≤ .05, ***P* < .01, *n* ≥ 3.

3.3. bFGF was identified as one of the cytokines upregulated in *Tgfb2^{Col1CreERT}* KO mice

We compared the expression profiles of cytokines and growth factors between the PC3-injected tibiae from *Tgfb2^{FloxE2}* and *Tgfb2^{Col1CreERT}* KO mice using cytokine array (Supplemental Fig. 3). Confirmed by enzyme-linked immunosorbent assay (ELISA), bFGF was the top up-regulated factor in PC3-injected tibiae from *Tgfb2^{Col1CreERT}* KO mice relative to those from *Tgfb2^{FloxE2}* or PBS-injected *Tgfb2^{Col1CreERT}* KO mice (Fig. 4A). Using IHC staining, we detected the increased bFGF prominently in cancer-associated osteoblasts (Fig. 4E). Using species specific PCR, we found that mouse, but not human, bFGF mRNA was increased in the PC3-injected, but not PBS-injected, *Tgfb2^{Col1CreERT}* KO tibiae (Fig. 4B–D). Thus, increased bFGF in cancer-associated osteoblasts was associated with PC3-injected tibiae from *Tgfb2^{Col1CreERT}* KO mice, which have larger bone lesion areas than those from the *Tgfb2^{FloxE2}* mice.

3.4. bFGF promoted osteoclastogenesis, inhibited osteoblastogenesis, but had no effect on PC3 viability in vitro

To delineate the effects of bFGF on tumor cells and bone cells, which are involved in PC3 bone lesion development, and also to determine whether the role of bFGF depends on osteoblast TGFBR2 expression. Osteoclasts were differentiated from the bone marrow cells of *Tgfb2^{Col1CreERT}* KO mice or *Tgfb2^{FloxE2}* mice. We found that cells exposed to bFGF had a dose-dependent, significant increase in osteoclastogenesis. Mature osteoclasts were identified as both TRAP-positive staining and the presence of at least three nuclei per cell (Fig. 5A). No differences in osteoclastogenesis between *Tgfb2^{FloxE2}* and *Tgfb2^{Col1CreERT}* KO mice were found with or without bFGF treatment. The data indicates that the osteoclastogenesis or bFGF-stimulated osteoclastogenesis were not dependent on the pre-exposed osteoblast TGF- β signaling effects.

We also found that bFGF inhibited osteoblastogenesis as

identified by positive ALP-staining cells (Fig. 5B). No significant differences in osteoblastogenesis were found between OB_Flox and OB_KO bone marrow cells with or without bFGF treatments, suggesting that cell autonomous TGF- β signaling did not significantly affect osteoblastogenesis or its inhibition by bFGF.

Furthermore, we found bFGF had no direct effect on PC3 cell viabilities at the doses (0.1–5.0 ng/ml) and time courses (24–48 h) examined (Fig. 5C).

3.5. bFGF mediated the increased PC3-bone lesions in *Tgfb2^{Col1CreERT}* KO mice

To determine the functional role of bFGF in PC3 bone lesion development in the context of TGFBR2 loss in osteoblast, we performed rescue studies. One day after PC3 intratibial injection, bFGF recombinant protein or BSA as vehicle control was given to the *Tgfb2^{FloxE2}* mice; neutralizing antibody for bFGF (Ab-bFGF) or control IgG was given to the *Tgfb2^{Col1CreERT}* KO mice (Fig. 6A). Significant increases in bone lesion areas were observed in the control IgG-treated *Tgfb2^{Col1CreERT}* KO mouse tibiae (KO_IgG) relative to those in BSA-treated *Tgfb2^{FloxE2}* mouse tibiae (Flox_BSA) at the 3rd week post PC3 injection. Moreover, we found that the Ab-bFGF treatment significantly decreased PC3 bone lesion areas in the *Tgfb2^{Col1CreERT}* KO mouse tibiae (KO_Ab group) relative to those of IgG treated mice (KO_IgG group). On the other hand, the recombinant bFGF treatment significantly increased PC3 bone lesion areas in *Tgfb2^{FloxE2}* mouse tibiae (Flox_bFGF versus Flox_BSA) (Fig. 6B and C). These rescue experiments showed that bFGF was mediating the increase in bone lesions caused by loss of TGF- β signaling in osteoblasts.

At cellular and molecular levels, we observed increases of PC3 tumor cell proliferation, cancer-associated fibroblasts (CAFs), and angiogenesis, as indicated by increases of p-HH3-positive cells, α -SMA-positive cells, and CD31 microvessel density, respectively, in the Flox_bFGF group relative to the Flox_BSA group. Furthermore,

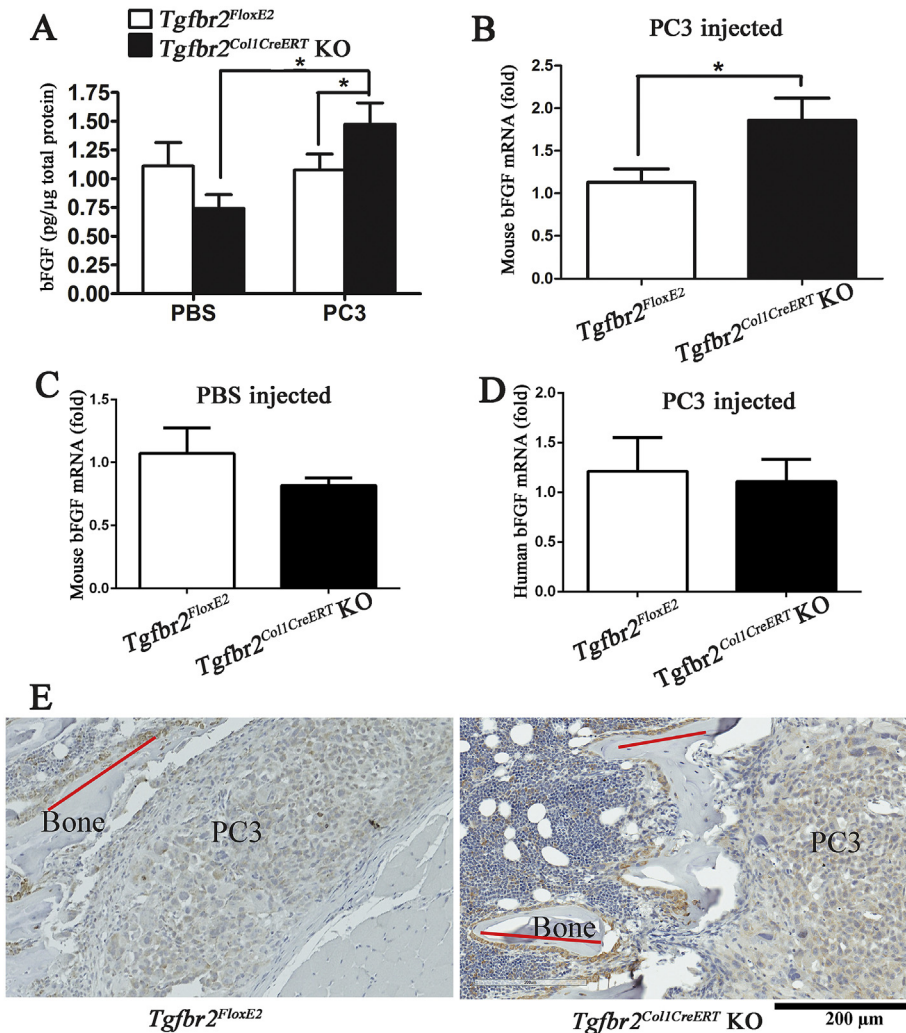


Fig. 4. bFGF expression was increased in osteoblasts of PC3 bone lesions in *Tgfb2*^{ColICreERT} KO mice. A) ELISA quantification of bFGF protein from crushed whole tibiae that had been injected with either PBS or PC3 cells. A significant increase of bFGF protein was detected in PC3-injected tibiae of *Tgfb2*^{ColICreERT} KO mice (relative to *Tgfb2*^{FloxE2} mice; two-way ANOVA, *P<.05). B–D) qRT-PCR analyses of the relative expression of species-specific bFGF mRNA from mouse tibiae. Mouse bFGF mRNA was significantly increased in PC3-injected tibiae of *Tgfb2*^{ColICreERT} KO mice (relative to *Tgfb2*^{FloxE2} mice; t-test, two-tailed, *P≤.05, n≥3). E) Representative IHC images of bFGF expression, which was increased in cancer-associated osteoblasts from *Tgfb2*^{ColICreERT} KO mice.

PC3 cell proliferation, microvessel density, and CAFs were decreased in the KO_Ab group relative to the KO_IgG group (Fig. 6D and E). Together, these data suggest that blocking bFGF reduces the increased PC3 bone lesions by loss of TGF-β signaling in osteoblasts, and this is associated with tumor cell proliferation, CAFs, and angiogenesis.

4. Discussion

In this study, we showed for the first time that loss of TGF-β signaling only in osteoblasts promoted PCa bone metastasis. Furthermore, we identified one of the factors, bFGF, which could mediate the function of loss of TGF-β signaling in osteoblasts in PC3-induced bone lesions. We showed that blocking bFGF using neutralizing antibody could inhibit the increased bone lesions by *Tgfb2* knockout in osteoblasts.

TGF-β signaling spatially and temporally controls cancer initiation, progression, and metastasis [14,15]. For example, loss of TGF-β signaling in prostate fibroblasts contributed to PCa initiation, castration resistance, and adhesion to bone matrix [13], [16–18]. On the other hand, myeloid TGF-β signaling was required for breast

and lung cancer metastasis to soft organs [19], as well as promoting breast cancer bone metastasis [12]. Therefore, more studies are needed in delineating the cell-specific role of TGF-β signaling and the underlying mechanism of actions. The significance of our current study is demonstrating a PCa bone metastasis-inhibition role of TGF-β signaling specifically in osteoblasts. Thus, this study revealed a concern for systemically blocking TGF-β signaling in bone metastasis. Consistent with previous reports [20–24], we did observe metastasis-promotion role of TGF-β signaling specifically in osteoclasts, suggesting that the effectiveness of systemically targeting TGF-β signaling blocked the metastasis-promoting role of TGF-β signaling in osteoclasts or/and in cancer cells. In order to achieve better efficiency of blocking TGF-β signaling in bone metastasis and discover new strategy eventually to treat patients, we will need to identify other targets that inhibit the metastasis-promoting effect from loss of TGF-β signaling in osteoblasts.

Our studies showed that bFGF was a surrogate in mediating the *Tgfb2*^{ColICreERT} KO increased PC3 bone lesions. bFGF belongs to the fibroblast growth factor family, which consists of 22 members. These ligands bind to the four FGF receptors, which are receptor tyrosine kinases (RTKs) [25,26]. Dysregulation of FGFs and FGFRs

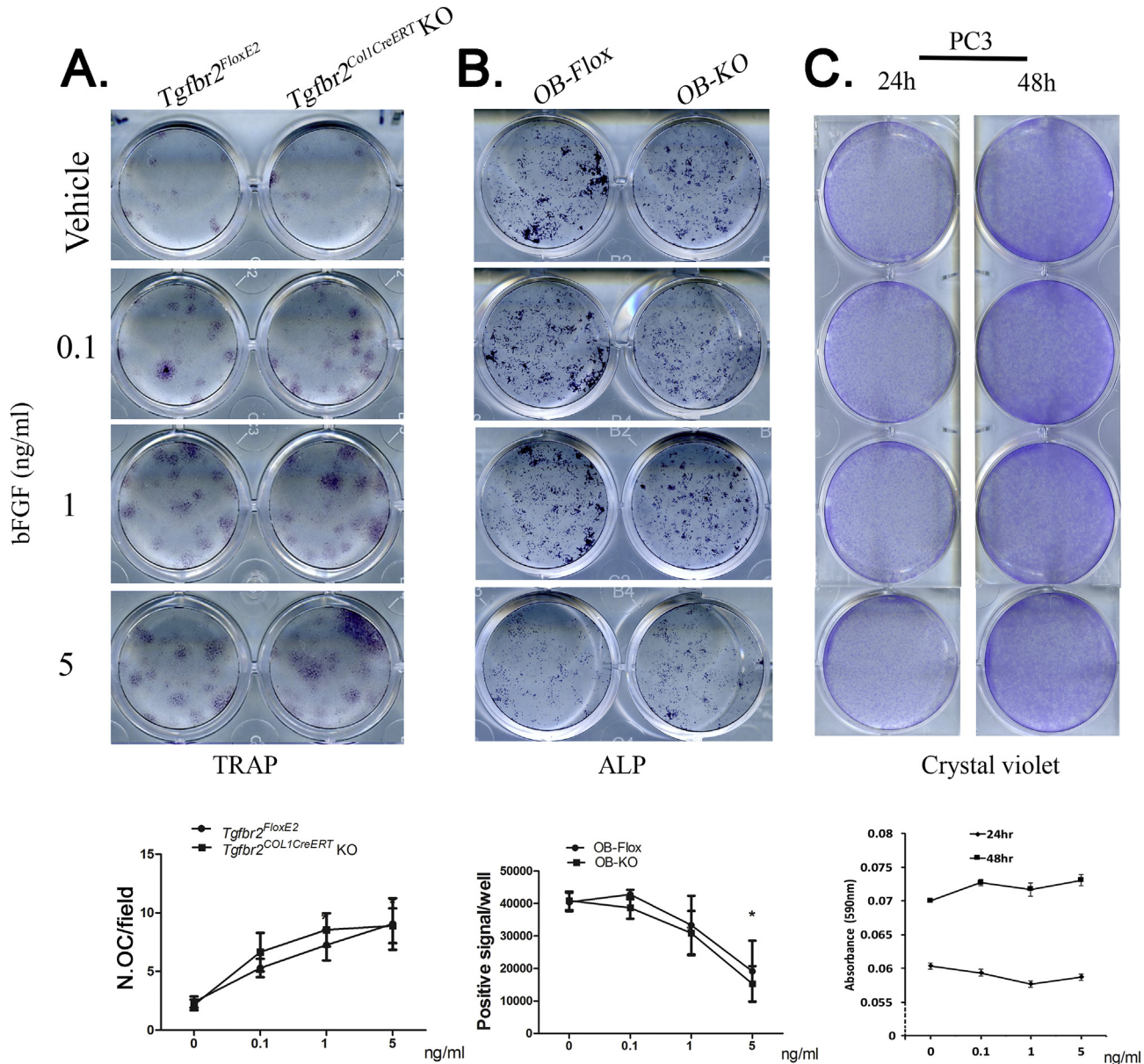


Fig. 5. bFGF promoted osteoclastogenesis, inhibited osteoblastogenesis, but had no effect on PC3 proliferation. Cells were exposed to bFGF at the doses and time points indicated. **A)** Representative TRAP staining and quantification for osteoclasts from *Tgfb2^{FlxEx2}* and *Tgfb2^{Col1CreERT} KO* littermates. A dose-dependent increase of osteoclast differentiation by bFGF was observed, but the effects of bFGF were not different between the cell lines. (two-way ANOVA, ***P<.001, n ≥ 3). **B)** Representative ALP staining and quantification for control osteoblasts (OB-Flox) and osteoblasts with deletion of the *Tgfb2* gene (OB-KO). A dose-dependent decrease of osteoblast differentiation by bFGF was observed, and the effects of bFGF were not different between OB-Flox and OB-KO (two-way ANOVA, ***P<.001, n ≥ 3). **C)** Representative images of PC3 cells stained with crystal violet. bFGF had no effect on PC3 cell proliferation after 24-h or 48-h treatment with various doses (one way ANOVA, n ≥ 3).

has been linked to the initiation, progression, and metastasis of many cancers, including PCa [26–30]. Blocking this axis by targeting the receptors has been actively investigated preclinically and clinically for many cancers and for bone metastasis, and most of these therapeutic efforts have targeted FGFRs [30–34]. However, one study has shown that most cancer cells could be rescued from anti-RTK drug sensitivity by simply exposing them to one or more RTK ligands; hepatocyte growth factor (HGF), FGF, and neuregulin 1 were the most broadly active ligands [35]. The RTK ligands could be produced by the cancer-associated cells in the tumor microenvironment such as CAFs and cancer-associated osteoblasts. In addition, despite some commonalities, each of the ligands has a unique effect and regulatory function. Therefore, neutralizing specific

ligands might be an alternate avenue for therapy. This treatment could be used alone or in combination with other therapies that target osteoclasts or PCa tumor cells. How does bFGF promote bone lesion development? We found that bFGF stimulated osteoclast differentiation and inhibited osteoblast differentiation. However, bFGF showed no direct effect on PC3 cell viabilities *in vitro*. Therefore, the increased tumor cell proliferation that was associated with bFGF upregulation in *Tgfb2^{Col1CreERT} KO* mouse tibiae could be an indirect effect of bFGF. Since the increases of tumor cell proliferation and bFGF were also associated with increased angiogenesis and CAF formation, we speculated an indirect effect of bFGF on tumor cell proliferation through angiogenesis and CAFs, and combining blocking bFGF and drugs that directly target tumor cells

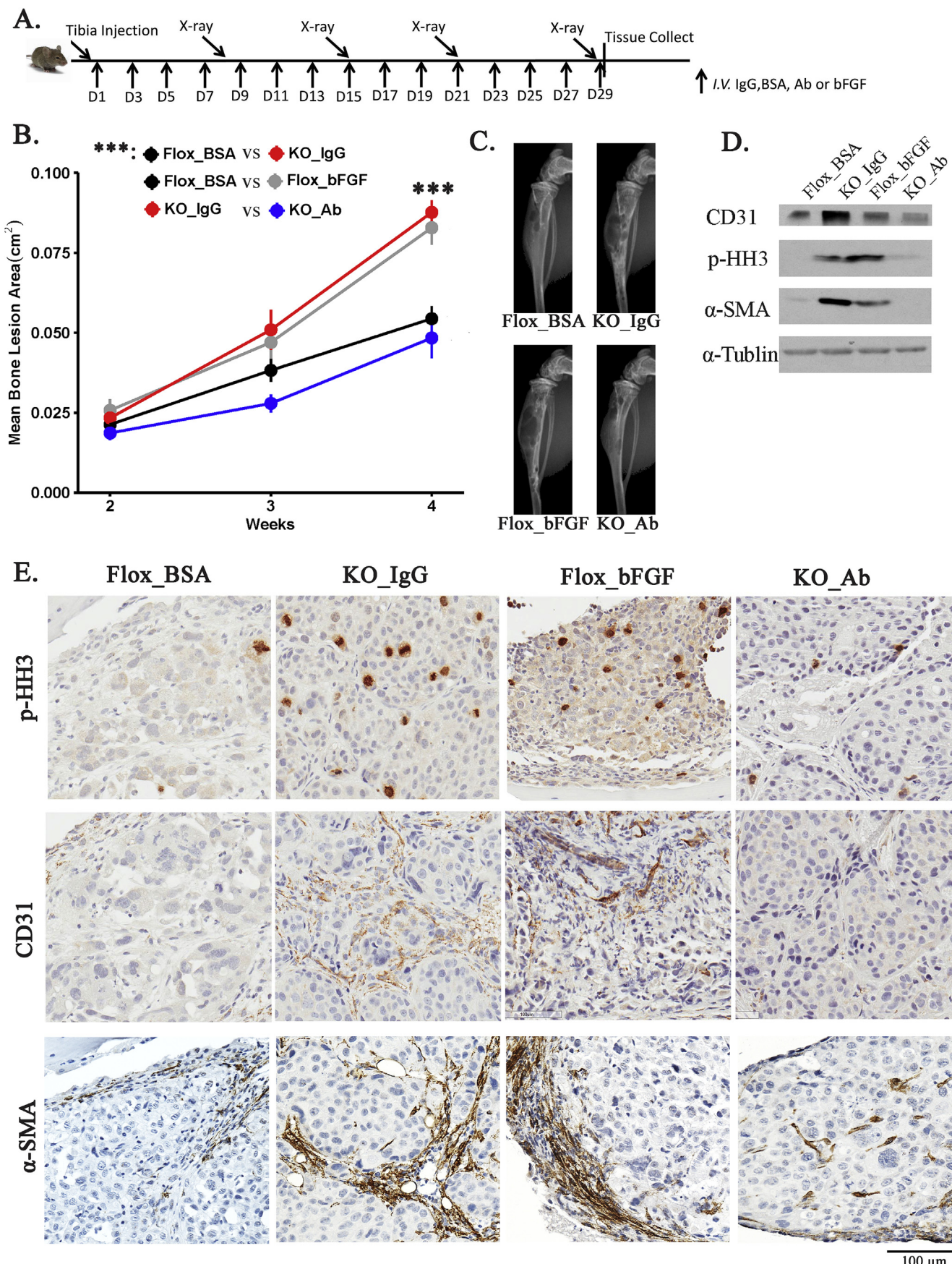


Fig. 6. bFGF mediated the increased PC3 bone lesions in *Tgfb2^{Col1CreERT}* KO mice. **A)** Schedule of the drug treatment, X-ray image acquisition, and end-point collection. **B)** Quantification of mean bone lesion area in PC3-injected mouse tibiae. Significant bone lesion development was found between the following pairs: Flox_BSA vs KO_IgG, Flox_BSA vs Flox_bFGF, and KO_IgG vs KO_Ab (linear mixed-effects model with a random intercept, *** $P < .001$, $n \geq 6$ tibiae). **C)** Representative X-ray images from each group at the final time point. **D)** Western blot analyses from whole tibiae harvested at the final time point. **E)** Representative images of IHC staining of p-HH3, CD31, and α -SMA.

could be a better approach for treating PCa bone metastasis. These will be tested in future studies.

In summary, our study revealed a metastasis-promoting role of the loss of TGF- β signaling specifically in osteoblasts and delineated the mechanism by which this specific loss promotes bone lesions, at least in part by bFGF. We determined the functional role of and the mechanism by which bFGF, a potential druggable target, mediated the metastasis-promoting effect contributed from osteoblasts.

Conflicts of interest statement

I, Xiaohong Li, the correspondent author of this manuscript, and represent all the other co-authors, Xiangqi Meng, Alexandra Vander Ark, Paul Daft, Erica Woodford, Jie Wang, and Zachary Madaj, declare that none of us has any conflict of interest on publishing this paper.

Grant support

The research was supported by DOD PCRP (W81XWH-12-1-0271 to X.L.) and Van Andel Research Institute Start-up funding (53010A to X.L.). X.M. is currently supported by the National Natural Science Foundation of China (No. 81702533).

Acknowledgments

We thank David Nadziejka for his technical editing of this manuscript. The content is solely the responsibility of the authors.

Appendix A. Supplementary data

Supplementary data related to this article can be found at <https://doi.org/10.1016/j.canlet.2018.01.018>.

References

- [1] R.E. Coleman, Clinical features of metastatic bone disease and risk of skeletal morbidity, *Clin. Cancer Res.* 12 (2006) 6243s–6249s, <https://doi.org/10.1158/1078-0432.CCR-06-0931>.
- [2] G.R. Mundy, Mechanisms of bone metastasis, *Cancer* 80 (1997) 1546–1556.
- [3] D. Padua, J. Massague, Roles of TGFbeta in metastasis, *Cell Res.* 19 (2009) 89–102, <https://doi.org/10.1038/cr.2008.316>.
- [4] J.T. Buijs, K.R. Stayrook, T.A. Guise, The role of TGF-beta in bone metastasis: novel therapeutic perspectives, *BoneKEy Rep.* 1 (2012) 96, <https://doi.org/10.1038/bonekey.2012.96>.
- [5] G.R. Mundy, Metastasis to bone: causes, consequences and therapeutic opportunities, *Nat. Rev. Cancer* 2 (2002) 584–593, <https://doi.org/10.1038/nrc867>.
- [6] G.D. Roodman, Mechanisms of bone metastasis, *N. Engl. J. Med.* 350 (2004) 1655–1664, <https://doi.org/10.1056/NEJMra030831>.
- [7] A. Hata, Y.G. Chen, TGF-beta signaling from receptors to smads, *Cold Spring Harb. Perspect. Biol.* 8 (2016), <https://doi.org/10.1101/cshperspect.a022061>.
- [8] J.K. Simmons, B.E. Hildreth 3rd, W. Supsavahad, S.M. Elshafae, B.B. Hassan, W.P. Dirksen, R.E. Toribio, T.J. Rosol, Animal models of bone metastasis, *Vet. Pathol.* 52 (2015) 827–841, <https://doi.org/10.1177/0300958515586223>.
- [9] Y. Shiozawa, E.A. Pedersen, A.M. Havens, Y. Jung, A. Mishra, J. Joseph, J.K. Kim, L.R. Patel, C. Ying, A.M. Ziegler, M.J. Pienta, J. Song, J. Wang, R.D. Loberg, P.H. Krebsbach, K.J. Pienta, R.S. Taichman, Human prostate cancer metastases target the hematopoietic stem cell niche to establish footholds in mouse bone marrow, *J. Clin. Invest.* 121 (2011) 1298–1312, <https://doi.org/10.1172/JCI43414>.
- [10] A. Chytil, M.A. Magnuson, C.V. Wright, H.L. Moses, Conditional inactivation of the TGF-beta type II receptor using Cre:Lox, *Genesis* 32 (2002) 73–75.
- [11] B. Zheng, Z. Zhang, C.M. Black, B. de Crombrugge, C.P. Denton, Ligand-dependent genetic recombination in fibroblasts : a potentially powerful technique for investigating gene function in fibrosis, *Am. J. Pathol.* 160 (2002) 1609–1617, [https://doi.org/10.1016/S0002-9440\(10\)61108-X](https://doi.org/10.1016/S0002-9440(10)61108-X).
- [12] X. Meng, A. Vander Ark, P. Lee, G. Hostetter, N.A. Bhowmick, L.M. Matrisian, B.O. Williams, C.K. Miranti, X. Li, Myeloid-specific TGF-beta signaling in bone promotes basic-FGF and breast cancer bone metastasis, *Oncogene* 35 (2016) 2370–2378, <https://doi.org/10.1038/onc.2015.297>.
- [13] X. Li, J.A. Sterling, K.H. Fan, R.L. Vessella, Y. Shyr, S.W. Hayward, L.M. Matrisian, N.A. Bhowmick, Loss of TGF-beta responsiveness in prostate stromal cells alters chemokine levels and facilitates the development of mixed osteoblastic/osteolytic bone lesions, *Mol. Cancer Res.* 10 (2012) 494–503, <https://doi.org/10.1158/1541-7786.MCR-11-0506>.
- [14] J. Massague, TGFbeta in cancer, *Cell* 134 (2008) 215–230, <https://doi.org/10.1016/j.cell.2008.07.001>.
- [15] H. Ikushima, K. Miyazono, TGFbeta signalling: a complex web in cancer progression, *Nat. Rev. Cancer* 10 (2010) 415–424, <https://doi.org/10.1038/nrc2853>.
- [16] X. Li, V. Placencia, J.M. Iturregui, C. Uwamariya, A.R. Sharif-Afshar, T. Koyama, S.W. Hayward, N.A. Bhowmick, Prostate tumor progression is mediated by a paracrine TGF-beta/Wnt3a signaling axis, *Oncogene* 27 (2008) 7118–7130, <https://doi.org/10.1038/onc.2008.293>.
- [17] V.R. Placencia, A.R. Sharif-Afshar, X. Li, H. Huang, C. Uwamariya, E.G. Neilson, M.M. Shen, R.J. Matusik, S.W. Hayward, N.A. Bhowmick, Stromal transforming growth factor-beta signaling mediates prostatic response to androgen ablation by paracrine Wnt activity, *Cancer Res.* 68 (2008) 4709–4718, <https://doi.org/10.1158/0008-5472.CAN-07-6289>.
- [18] N.A. Bhowmick, A. Chytil, D. Plieth, A.E. Gorska, N. Dumont, S. Shappell, M.K. Washington, E.G. Neilson, H.L. Moses, TGF-beta signaling in fibroblasts modulates the oncogenic potential of adjacent epithelia, *Science* 303 (2004) 848–851, <https://doi.org/10.1126/science.1090922>.
- [19] Y. Pang, S.K. Gara, B.R. Achyut, Z. Li, H.H. Yan, C.P. Day, J.M. Weiss, G. Trinchieri, J.C. Morris, L. Yang, TGF-beta signaling in myeloid cells is required for tumor metastasis, *Cancer Discov.* 3 (2013) 936–951, <https://doi.org/10.1158/2159-8290.CD-12-0527>.
- [20] S. Ehata, A. Hanyu, M. Fujime, Y. Katsuno, E. Fukunaga, K. Goto, Y. Ishikawa, K. Nomura, H. Yokoo, T. Shimizu, E. Ogata, K. Miyazono, K. Shimizu, T. Imamura, Ki26894, a novel transforming growth factor-beta type I receptor kinase inhibitor, inhibits *in vitro* invasion and *in vivo* bone metastasis of a human breast cancer cell line, *Cancer Sci.* 98 (2007) 127–133, <https://doi.org/10.1111/j.1349-7006.2006.00357.x>.
- [21] A. Bandyopadhyay, J.K. Agyin, L. Wang, Y. Tang, X. Lei, B.M. Story, J.E. Cornell, B.H. Pollock, G.R. Mundy, L.Z. Sun, Inhibition of pulmonary and skeletal metastasis by a transforming growth factor-beta type I receptor kinase inhibitor, *Cancer Res.* 66 (2006) 6714–6721, <https://doi.org/10.1158/0008-5472.CAN-05-3565>.
- [22] S. Biswas, J.S. Nyman, J. Alvarez, A. Chakrabarti, A. Ayres, J. Sterling, J. Edwards, T. Rana, R. Johnson, D.S. Perrien, S. Lonning, Y. Shyr, L.M. Matrisian, G.R. Mundy, Anti-transforming growth factor ss antibody treatment rescues bone loss and prevents breast cancer metastasis to bone, *PLoS One* 6 (2011), e27090, <https://doi.org/10.1371/journal.pone.0027090>.
- [23] J.J. Yin, K. Selander, J.M. Chirgwin, M. Dallas, B.G. Grubbs, R. Wieser, J. Massague, G.R. Mundy, T.A. Guise, TGF-beta signaling blockade inhibits PI(THr1) secretion by breast cancer cells and bone metastases development, *J. Clin. Invest.* 103 (1999) 197–206, <https://doi.org/10.1172/JCI3523>.
- [24] P.G. Fournier, P. Juarez, G. Jiang, G.A. Clines, M. Niewolna, H.S. Kim, H.W. Walton, X.H. Peng, Y. Liu, K.S. Mohammad, C.D. Wells, J.M. Chirgwin, T.A. Guise, The TGF-beta signaling regulator PMEPA1 suppresses prostate cancer metastases to bone, *Cancer Cell* 27 (2015) 809–821, <https://doi.org/10.1016/j.ccr.2015.04.009>.
- [25] C.J. Powers, S.W. McLeskey, A. Wellstein, Fibroblast growth factors, their receptors and signaling, *Endocr. Relat. Cancer* 7 (2000) 165–197.
- [26] N. Turner, R. Grose, Fibroblast growth factor signalling: from development to cancer, *Nat. Rev. Cancer* 10 (2010) 116–129, <https://doi.org/10.1038/nrc2780>.
- [27] T. Murphy, S. Darby, M.E. Mathers, V.J. Gnanapragasam, Evidence for distinct alterations in the FGF axis in prostate cancer progression to an aggressive clinical phenotype, *J. Pathol.* 220 (2010) 452–460, <https://doi.org/10.1002/path.2657>.
- [28] M.P. Valta, J. Tuomela, A. Bjartell, E. Valve, H.K. Vaananen, P. Harkonen, FGF-8 is involved in bone metastasis of prostate cancer, *Int. J. Cancer* 123 (2008) 22–31, <https://doi.org/10.1002/ijc.23422>.
- [29] F. Yang, Y. Gao, J. Geng, D. Qu, Q. Han, J. Qi, G. Chen, Elevated expression of SOX2 and FGFR1 in correlation with poor prognosis in patients with small cell lung cancer, *Int. J. Clin. Exp. Pathol.* 6 (2013) 2846–2854.
- [30] X. Wan, P.G. Corn, J. Yang, N. Palanisamy, M.W. Starbuck, E. Efstatithou, E.M. Li Ning Tapia, A.J. Zurita, A. Aparicio, M.K. Ravoori, E.S. Vazquez, D.R. Robinson, Y.M. Wu, X. Cao, M.K. Iyer, W. McKeehan, V. Kundra, F. Wang, P. Troncoso, A.M. Chinnaiyan, C.J. Logothetis, N.M. Navone, Prostate cancer cell-stromal cell crosstalk via FGFR1 mediates antitumor activity of dovitinib in bone metastases, *Sci. Translat. Med.* 6 (2014), <https://doi.org/10.1126/scitranslmed.3009332>, 252ra122.
- [31] F. Li, H. Huynh, X. Li, D.A. Ruddy, Y. Wang, R. Ong, P. Chow, S. Qiu, A. Tam, D.P. Rakiec, R. Schlegel, J.E. Monahan, A. Huang, FGFR-mediated reactivation of MAPK signalling attenuates antitumor effects of imatinib in gastrointestinal stromal tumors, *Cancer Discov.* 5 (2015) 438–451, <https://doi.org/10.1158/2159-8290.CD-14-0763>.
- [32] K. Azuma, A. Kawahara, K. Sonoda, K. Nakashima, K. Tashiro, K. Watari, H. Izumi, M. Kage, M. Kuwano, M. Ono, T. Hoshino, FGFR1 activation is an escape mechanism in human lung cancer cells resistant to afatinib, a pan-EGFR family kinase inhibitor, *Oncotarget* 5 (2014) 5908–5919, <https://doi.org/10.18632/oncotarget.1866>.
- [33] M. Hagel, C. Miduturu, M. Sheets, N. Rubin, W. Weng, N. Stransky, N. Bifulco, J.L. Kim, B. Hodous, N. Brooijmans, A. Shutes, C. Winter, C. Lengauer, N.E. Kohl, T. Guzi, First selective small molecule inhibitor of FGFR4 for the treatment of

- hepatocellular carcinomas with an activated FGFR4 signaling pathway, *Cancer Discov.* 5 (2015) 424–437, <https://doi.org/10.1158/2159-8290.CD-14-1029>.
- [34] F. Bono, F. De Smet, C. Herbert, K. De Bock, M. Georgiadou, P. Fons, M. Tjwa, C. Alcouffe, A. Ny, M. Bianciotto, B. Jonckx, M. Murakami, A.A. Lanahan, C. Michielsen, D. Sibrac, F. Dol-Gleizes, M. Mazzone, S. Zacchigna, J.P. Herault, C. Fischer, P. Rigon, C. Ruiz de Almodovar, F. Claes, I. Blanc, K. Poesen, J. Zhang, I. Segura, G. Gueguen, M.F. Bordes, D. Lambrechts, R. Broussy, M. van de Wouwer, C. Michaux, T. Shimada, I. Jean, S. Blacher, A. Noel, P. Motte, E. Rom, J.M. Rakic, S. Katsuma, P. Schaeffer, A. Yayon, A. Van Schepdael, H. Schwalbe, F.L. Gervasio, G. Carmeliet, J. Rozensky, M. Dewerchin, M. Simons, A. Christopoulos, J.M. Herbert, P. Carmeliet, Inhibition of tumor angiogenesis and growth by a small-molecule multi-FGF receptor blocker with allosteric properties, *Cancer Cell* 23 (2013) 477–488, <https://doi.org/10.1016/j.ccr.2013.02.019>.
- [35] T.R. Wilson, J. Fridlyand, Y.B. Yan, E. Penuel, L. Burton, E. Chan, J. Peng, E. Lin, Y.L. Wang, J. Sosman, A. Ribas, J. Li, J. Moffat, D.P. Sutherland, H. Koeppen, M. Merchant, R. Neve, J. Settleman, Widespread potential for growth-factor-driven resistance to anticancer kinase inhibitors, *Nature* 487 (2012) 505–U1652, <https://doi.org/10.1038/nature11249>.